

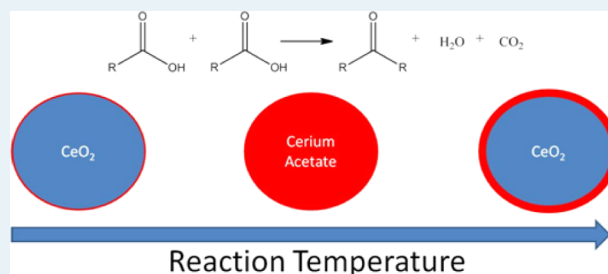
# Insights into the Ceria-Catalyzed Ketonization Reaction for Biofuels Applications

Ryan W. Snell and Brent H. Shanks<sup>\*,†</sup>

<sup>†</sup>Department of Chemical and Biological Engineering, Iowa State University, 1140L BRL, Ames, Iowa, 50011, United States

## S Supporting Information

**ABSTRACT:** The ketonization of small organic acids is a valuable reaction for biorenewable applications. Ceria has long been used as a catalyst for this reaction; however, under both liquid and vapor phase conditions, it was found that given the right temperature regime of about 150–300 °C, cerium oxide, which was previously believed to be a stable catalyst for ketonization, can undergo bulk transformations. This result, along with other literature reports, suggest that the long held belief of two separate reaction pathways for either bulk or surface ketonization reactions are not required to explain the interaction of cerium oxide with organic acids. X-ray photon spectroscopy, scanning electron microscopy, and temperature programmed decomposition results supported the formation of metal acetates and explained the occurrence of cerium reduction as well as the formation of cerium oxide/acetate whiskers. After thermogravimetry/mass spectrometry and FT-IR experiments, a single reaction sequence is proposed that can be applied to either surface or bulk reactions with ceria.



**KEYWORDS:** ketonization, cerium oxide, acetic acid, metal carboxylate, bio-oil

## 1. INTRODUCTION

Although a number of renewable energy alternatives, such as solar and wind, are increasingly being utilized, there remains a tremendous challenge in replacing a trillion dollar infrastructure built around liquid fuels. Therefore, the creation of a renewable liquid fuel able to successfully make use of the current infrastructure would be extremely valuable. Because biomass provides a renewable source of carbon, it is a potential alternative to current petroleum use. Although there are a number of different techniques being explored for converting biomass to liquid fuels, fast pyrolysis has been increasingly discussed because of the simplicity of the process, direct creation of a liquid bio-oil, and the flexibility to use different feedstocks.<sup>1</sup> However, there are a number of undesirable characteristics of this oil, such as a low pH and high oxygen content, both caused in part by its large quantity of small organic acids.<sup>2</sup> Since bio-oil contains a number of thermally unstable compounds, it would be preferred to perform condensed phase catalytic reactions so as to address some of these issues.

One reaction that would be potentially beneficial is ketonization. The ketonization reaction has been attracting increasing attention for biorenewable fuel applications since Kunkes et al. reported its use during the conversion of glucose to liquid fuels.<sup>3</sup> Regrettably, the high temperatures, typically >300 °C, utilized for the reaction make it impractical for condensed phase applications, as would be preferred with bio-oil. Increasing catalyst activity is thus vital for obtaining reasonable liquid phase reaction conditions. To achieve this task, it would be helpful to have a good understanding of the

underlying chemistry involved in the reaction. Unfortunately, despite recent advances, much about ketonization remains debated, including the catalytic mechanism.<sup>4,5</sup> This is particularly true regarding the reaction in the condensed phase.

Adding to the challenge of understanding the ketonization reaction is the postulate that the reaction proceeds through different mechanisms, depending on the metal oxide catalyst used.<sup>4,6</sup> For metal oxide catalysts with a low metal–oxygen bond strength or low lattice energy, the reaction purportedly progresses through the formation of a bulk metal carboxylate, which then acts as the working catalyst and whose thermal decomposition results in ketone production. In contrast, for catalysts with a high metal–oxygen bond strength or large lattice energy, a surface-catalyzed reaction is reported to promote the formation of the ketone.<sup>4</sup> For reference, the value of the lattice energy for ceria relative to other potential ketonization catalysts is given in Table 1. However, Mekhemer et al. reported that MgO could catalyze the ketonization reaction through either bulk or surface reactions, depending on the temperature. They reported that MgO underwent transformation to a bulk acetate during room temperature exposure to acetic acid while higher temperatures favored a reaction proceeding through surface adsorption.<sup>7</sup> This apparent deviation from the earlier suggested lattice-energy-directed, two-pathway model was proposed to occur in this particular instance because of the unique basicity of the oxide. Given

Received: January 2, 2013

Revised: March 4, 2013

Published: March 8, 2013

**Table 1. Lattice Energies of Potential Ketonization Catalysts<sup>8</sup>**

material	lattice energy (kJ/mol)
Al <sub>2</sub> O <sub>3</sub>	15916
Cr <sub>2</sub> O <sub>3</sub>	15276
MnO <sub>2</sub>	12970
TiO <sub>2</sub>	12150
ZrO <sub>2</sub>	11188
CeO <sub>2</sub>	9627
BeO	4514
ZnO	4142
MgO	3795
PbO	3520
CaCO <sub>3</sub>	2804

these results, the authors proposed that the reaction mechanism was different for low-temperature ketonization, which purportedly progressed through the pyrolytic route, from that at high temperatures, which catalyzed the reaction through the use of both acid and base surface sites.<sup>7</sup>

In a large screening study of metal oxides in the ketonization reaction, ceria was found to be a ketonization catalyst superior to MgO,<sup>9</sup> and ceria has been the focus of a number of studies.<sup>10–14</sup> Because we were interested in exploring ketonization at lower temperatures in the condensed phase, a high-activity catalyst was desirable, so the focus in the current work was how the reaction of the model bio-oil compound, acetic acid, proceeded in the presence of ceria.<sup>9</sup> In particular, we examined the question of bulk transformation versus surface adsorption for ceria.

## 2. RESULTS AND DISCUSSION

**2.1. Formation of Cerium Acetate.** The synthesized ceria used in the reaction studies was first characterized in its fresh state. The material, which had a BET surface area of 73 m<sup>2</sup>/g, was found from X-ray diffraction (XRD) to be in the cerianite form (Figure S1, Supporting Information). Consistent with the XRD results, X-ray photoelectron spectroscopy (XPS) analysis showed that the cerium oxidation state was primarily Ce<sup>4+</sup> (Supporting Information Figure S2). From scanning electron spectroscopy (SEM) images (Supporting Information Figure S3), the ceria particles were in the form of nonuniformly shaped agglomerated crystals.

The primary focus of the current work was exploring lower temperatures that could be utilized for reaction in the condensed phase. As shown in Figure 1, the acetic acid ketonization reaction proceeded in toluene, even at the comparatively low temperature of 230 °C. From exploring

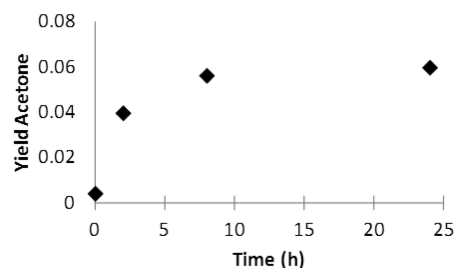


**Figure 1.** Ketonization of acetic acid indicating that the reaction can proceed at low temperatures (230 °C, 50 mL of toluene, 1.0 g of acetic acid, 0.055 g of ceria).

different reaction temperatures, it was found that at 150 °C, only traces of acetone were observed after 24 h using an acid/ceria ratio of 5, but increasing the reaction temperature to 300 °C led to complete conversion of the acetic acid in 30 min.

A number of reports in which the ketonization reaction was performed at temperatures above 300 °C have reported that the structure of the ceria catalyst was stable during the ketonization reaction, as determined by postreaction characterization using XRD.<sup>6,13,15</sup> However, in the current work, postreaction XRD characterization of the ceria catalyst used at 230 °C demonstrated that the oxide underwent bulk restructuring during the course of the reaction. Further reactions were run to see if this crystal structure change would occur at lower temperatures, as was found by Mekhemer et al. with MgO.<sup>7</sup> Interestingly, the original fluorite phase for the ceria was maintained when exposed to acetic acid at temperatures lower than 200 °C, demonstrating that bulk absorbance of the acid was not occurring at these temperatures. In addition, the fluorite crystal structure was preserved when the ceria was used at a reaction temperature of 300 °C. Therefore, as shown in Figure 2 for the postreaction ceria, there appeared to be an

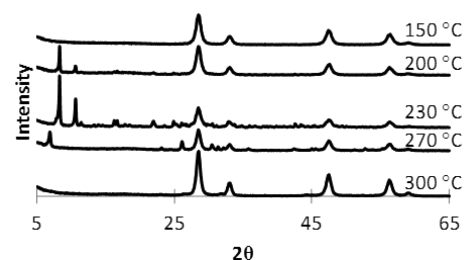


**Figure 2.** XRD figures of postreaction ceria catalysts used at different temperatures in the ketonization of acetic acid (1.0 g of acetic acid, 24 h, 0.20 g of catalyst).

intermediate temperature range during which ceria restructuring occurred. It has been proposed that metal oxide catalysts with metal–oxygen bonds weak enough to undergo bulk carboxylate formation have low activity in ketonization.<sup>16</sup> However, these results appeared to contradict this postulate because ceria, one of the most active ketonization catalysts, was clearly found to undergo bulk crystal changes. To validate that this change in the bulk structure was due to interaction with acetic acid and not a solvent effect, a control was performed in which no acetic acid was added. In this experiment, no bulk rearrangement occurred, which unquestionably demonstrated the requirement of acetic acid interaction with ceria to cause the bulk transformation.

To further confirm that bulk metal acetate was being formed during the course of the reaction, a temperature-programmed decomposition (TPD) experiment was performed in which the spent catalyst was heated at a 5 °C/min ramp rate and the evolved products were measured through the use of mass spectrometry. As shown in Figure 3, acetone was evolved in two steps, the first beginning at ~250 °C and reaching a maximum at ~300 °C, which was near the temperatures that the ketonization reaction readily occurred. To provide a comparison, TPD was also performed with purchased cerium acetate hydrate. Figure 4 demonstrates that a similar evolution of products was found for cerium acetate, and the acetone evolution appeared to occur at approximately the same temperatures. The one slight difference with the cerium acetate hydrate was the appearance of three acetone evolution peaks, as

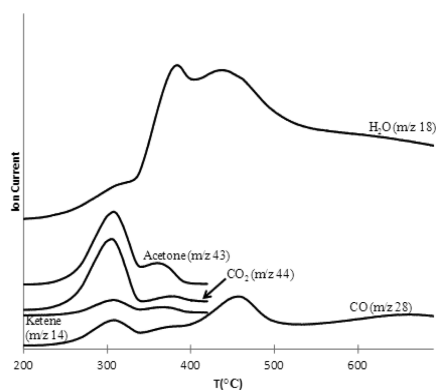


**Figure 3.** TPD of cerium oxide catalyst after use for 24 h in the ketonization of acetic acid at 230 °C.

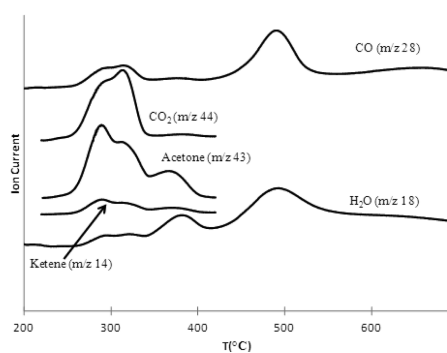


**Figure 4.** TPD of cerium acetate hydrate.

opposed to the two observed with the spent catalyst. A possible cause for this difference may be that the spent ceria catalyst was not fully transformed into bulk acetate, as seen in Figure 2, and instead was in an intermediate cerium oxyacetate form. Because the catalyst used at 300 °C did not show the bulk restructuring during the course of reaction as determined by XRD, TPD was performed on this used catalyst to see whether acetone would be evolved at similar temperatures. As shown in Figure 5, this result was, indeed, the case.

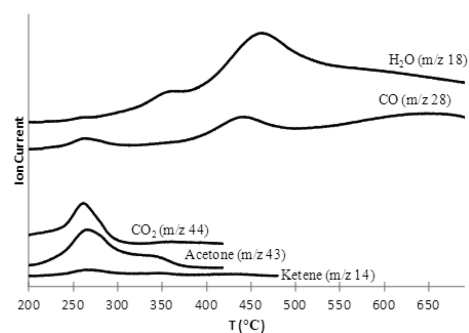


**Figure 5.** Ceria catalyst TPD profile after being used in the ketonization of acetic acid at 300 °C for 30 min.

XRD of the cerium acetate hydrate sample did not result in a diffractogram that was equivalent to that found with the ceria catalyst used at 230 °C, which supported the observation that during the course of the reaction, ceria was not transformed into a pure carboxylate but, instead, some apparent intermediate form. To further explore the possible connection, both cerium acetate hydrate and cerium carbonate hydrate were

exposed to the same reaction conditions as was the ceria. After this exposure, both the cerium acetate hydrate and cerium carbonate hydrate were found to yield diffractograms very similar to that of the postreaction ceria, lending more evidence to the formation of a metal–carboxylate intermediate during ceria catalyzed ketonization (Figure 6).

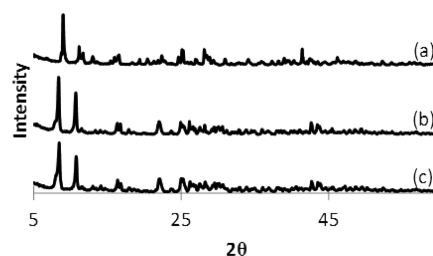


**Figure 6.** XRD figures of (a) fresh cerium acetate hydrate, (b) reaction exposed cerium acetate, and (c) reaction-exposed cerium carbonate hydrate (0.85 or 1.0 g of acetic acid for acetate or carbonate, 2 h reaction, 230 °C, 0.28 g of cerium acetate, 0.20 g of cerium carbonate).

SEM imaging of the ceria catalyst used at 230 °C showed the formation of large rods or whiskers (Figure 7). A control in

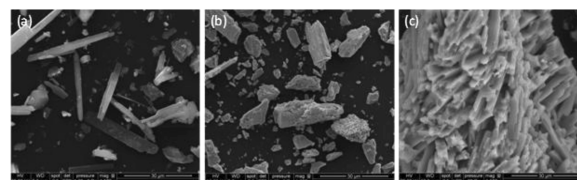


**Figure 7.** SEM images of ceria catalysts after use in (a) 24 h reaction with an acid/catalyst weight ratio of 18.1, 230 °C, 50 mL of toluene (b) 24 h and 230 °C in toluene solvent, and (c) cerium acetate hydrate after use in reaction with an acid/acetate weight ratio of 3.1, 2 h reaction, 230 °C, 50 mL of toluene.

which ceria was exposed to the reaction conditions without the presence of acetic acid demonstrated that this restructuring was growth promoted not by the solvent but, rather, through interaction with the acetic acid. Interestingly, the cerium acetate hydrate when used under reaction conditions in the presence of acetic acid also displayed the formation of rods, but in this case, the rods were significantly aggregated. The SEM results complemented and corroborated the previous XRD and TPD findings in that some form of metal carboxylate was being formed at the intermediate reaction temperatures.

Because reports on the ketonization of small organic acids have almost exclusively been performed in the gas phase as a result of the high temperatures being used, it was evaluated whether the condensed phase results were unique to this phase or were more generally applicable to the reaction independent of the reaction phase. To probe this question, in situ XRD was used in which acetic acid vapors were passed over the ceria catalyst at different temperatures while continuously scanning over a specified  $2\theta$  range. The results are shown in Figure 8. As the sample was taken through the different temperature regimes, bulk acetate formation was observed, demonstrating that the phase change behavior of the ceria when exposed to acetic acid in the gas phase was similar to that seen in the condensed phase. Taken together, the results from examining behavior in either reaction phase suggested that acetate formation occurred independently of the reaction phase within

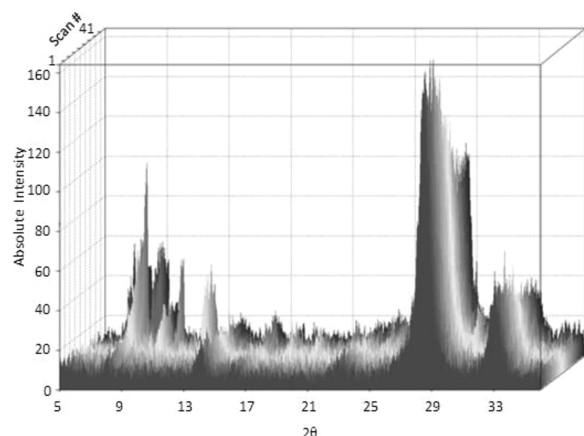


**Figure 8.** In situ XRD characterization of ceria behavior during the course of acetic acid vapor phase ketonization at various temperatures. Temperatures were increased after every 9 scans so that scans 1–9, 10–18, 19–27, 28–36, and 36–45 occurred at temperatures of 150, 200, 230, 270, and 300 °C, respectively.

the temperature window of  $\sim 200$ – $300$  °C. Of note from Figure 8 was that at 300 °C (scans 36–45), the diffractogram had not reverted back to the original ceria form, as might be expected from the results shown in Figure 2.

To explore this apparent difference, a condensed phase reaction was performed at 230 °C with 1.0 g of acetic acid and 0.20 g of ceria for 24 h. After reaction, the catalyst was separated and analyzed by XRD, and then the postreaction ceria catalyst was placed in toluene and held for 1 h at 300 °C. Following this treatment, the ceria was again separated and analyzed by XRD, with the results compared with a catalyst exposed to reaction conditions at 300 °C for 30 min with 1.0 g of acetic acid, and 0.2 g of ceria. Figure 9 shows that results

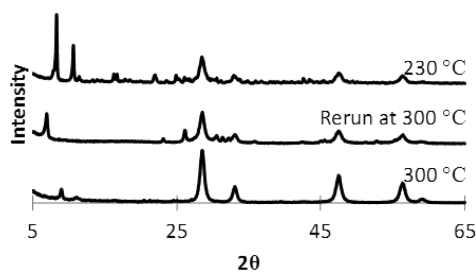


**Figure 9.** XRD profiles of ceria exposed to 24 h reactions at 230 °C, rerunning after the catalyst was placed in toluene at 300 °C for 1 h, and ceria after only 30 min of reaction at 300 °C.

found in the condensed phase were analogous to those discovered in the vapor phase. For the experiments in both phases, the ceria did not revert back to its original crystal structure at 300 °C after the initial formation of metal carboxylates in the bulk. However, as shown in Figure 2 and Supporting Information Figure S4, when ceria was exposed to acetic acid in either the liquid or vapor phase at 300 °C, the material did not show the formation of a bulk metal carboxylate. Since previously reported research examining the stability of ceria in the ketonization reaction was performed at temperatures at or greater than 300 °C, the lack of bulk transformation would be expected.<sup>9,13</sup>

From the results in the current work, it is apparent that the lack of carboxylate formation in the bulk at high temperatures is

not the result of metal–oxygen bond strength differences. Therefore, this material property alone does not dictate the route for the ketonization reaction pathway. Furthermore, recent reports have shown that oxides with even higher lattice energies than ceria such as  $\text{La}_2\text{O}_3$  and  $\text{Nd}_2\text{O}_3$  undergo partial bulk acetate formation during ketonization of acetic acid, but ceria did not.<sup>13</sup> The reason that ceria was found to be stable in the study was likely due to the high reaction temperature being used. It is worth considering whether two different reaction pathways are required to reconcile previously reported ketonization results. It is well-known that the pyrolysis of select metal acetates leads to the formation of acetone;<sup>17</sup> however, clear evidence that the surface mechanism is catalytic and different from the bulk thermal decomposition mechanism is not as apparent.

It is possible the proposed surface catalytic pathway is just the result of surface carboxylate pyrolysis. This hypothesis would explain the ceria XRD observations in Figure 2. At high temperatures, metal carboxylate formation in the bulk would not occur because of the thermal instability of this species at these conditions. Moreover, properties of the particular metal oxide, such as its lattice energy, could prevent the formation of carboxylates in the bulk until sufficient energy is available to break M–O bonds in the metal oxide. If the reaction temperature required to break M–O bonds and form carboxylates in the bulk is higher than the value for which the metal carboxylate decomposes, then disruption of the crystal structure would not be observed. However, this situation does not require different reaction mechanisms because the metal carboxylates could still form on the surface or, depending on transport limitations, possibly even within the first few atomic layers. After formation, these carboxylates could pyrolytically decompose to form the ketone. Hence, in either the bulk or surface-promoted cases, a necessary intermediate species would be a metal carboxylate. A schematic diagram depicting this hypothesis for ceria is shown in Figure 10.

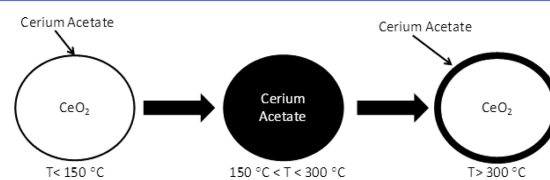


**Figure 10.** Different temperature regimes for ceria-catalyzed ketonization. At low temperatures, there is insufficient energy for the acetic acid to break the Ce–O bonds; at intermediate temperatures, acetates are able to form but are stable enough to form carboxylates in the bulk; and at high temperatures, acetates form but are rapidly decomposed to form acetone, leaving the bulk structure maintained.

**2.2. Decomposition of Cerium Carboxylates.** It has been commonly reported that an  $\alpha$ -hydrogen is necessary for ketonization to proceed, which lends support to the formation of a ketene-like intermediate.<sup>4,18</sup> To examine whether this concept would fit into the hypothesis of thermal carboxylate decomposition, the ketonization of pivalic acid (trimethylacetic acid) was attempted in the condensed phase. Consistent with the literature, none of the expected ketonization product (2,2,4,4-tetramethyl-3-pentanone) was found at temperatures of up to 315 °C in 24 h reaction runs (1.7 g of pivalic acid, 0.2 g of catalyst). Moreover, when the postreaction ceria catalyst was separated from the reaction mixture using vacuum filtration and



analyzed by XRD at temperatures up to 300 °C, the original cerianite structure was maintained. In contrast, when the ketonization reaction was run at 315 °C, no catalyst powder could be observed in the reaction mixture post reaction. After drying in air to remove the solvent and reactant, a powder precipitate was formed. Averaging over four EDS spectra, the content of Ce, C, and O in the powder were found to be 39, 43, and 17 wt %, respectively. This composition is approximately that of cerium(III) pivalate (34% Ce, 43% C, 23% O). The electron-donating methyl groups or sterics of pivalic acid could explain the higher temperature necessary for bulk carboxylate formation when ceria was exposed to pivalic acid. SEM images of the recovered precipitate from the reaction did not show rod-shaped morphology (see Supporting Information Figure S5), as was evident for the ceria after reaction with acetic acid. This result was reasonable because cerium pivalate is readily soluble in toluene, but cerium acetate is not.

XPS of the precipitate sample (Supporting Information Figure S6) showed the cerium, which was in the  $Ce^{4+}$  state prior to reaction, had been fully reduced to  $Ce^{3+}$  in the course of cerium pivalate formation. The observation of metal ion reduction might explain some reports of cerium reduction during the course of ketonization by demonstrating that reduction of the metal oxide occurred during carboxylate formation and not necessarily during evolution or further reactions of the ketone.<sup>19,20</sup> This explanation would be consistent with our XPS characterization of the postreaction ceria. The material was dried in air at 100 °C, which would likely oxidize any reduced oxide that had formed; however, the bulk cerium carboxylate formation could stabilize the cerium in the 3+ state and would not decompose in air at the low temperature used for drying.

The observation that no pivalic acid ketonization over cerium oxide occurred at temperatures up to 315 °C in the condensed phase was consistent with the proposed need for an  $\alpha$ -hydrogen. It has been shown previously that branching and, thus, a loss in the number of  $\alpha$ -hydrogen atoms for a given acid compound decreases its activity in the ketonization reaction,<sup>18</sup> so the thermal stability of metal carboxylates should increase in the order of acetate < propionate < isobutyrate < pivalate. Figure 11 shows the decomposition behavior of the respective

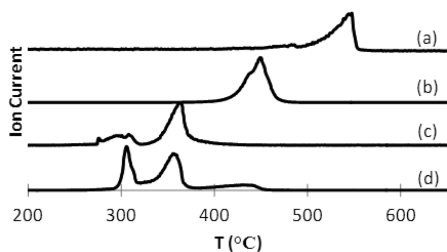


**Figure 11.** Normalized MS results obtained during the thermogravimetric analysis of cerium carboxylates with different degrees of branching (a) cerium pivalate  $m/z = 58$ , (b) cerium isobutyrate  $m/z = 71$ , (c) cerium propionate  $m/z = 86$ , and (d) cerium acetate  $m/z = 58$ .

cerium carboxylates as measured by thermogravimetry/mass spectrometry. The relative decomposition order followed exactly what was expected in which substitution of methyl groups for the  $\alpha$ -hydrogens dramatically increased the stability of the carboxylate. Cerium acetate, propionate, and isobutyrate decomposed and formed their corresponding ketones. However, it was difficult to probe the ketone formation for cerium

pivalate because it was not decomposed until such a high temperature that the formed ketone decomposed immediately. These results suggested that the necessity of an  $\alpha$ -hydrogen could actually be related more to a pyrolytic mechanism than a catalytic mechanism.

**2.3. Proposed Acetic Acid Ketonization Reaction Sequence with Ceria.** Kinetic modeling of the ketonization reaction has shown that Langmuir–Hinshelwood kinetics with two adsorbed species reacting result in a good fit with experimental data.<sup>21,22</sup> Carboxylate species can bind with metal cations in a number of different conformations.<sup>23</sup> The type of binding may influence the ease with which the intermediate metal acetate is thermally decomposed. Metal acetate infrared spectra and its connection to carboxylate coordination has previously been studied.<sup>24</sup> Differences in carboxylate bond symmetry were found to occur depending on the type of binding, that is, unidentate, bidentate, or ionic. These differences create varying locations for the  $\nu_{\text{asym}}(\text{CO}_2)$  and  $\nu_{\text{sym}}(\text{CO}_2)$  bands, thus changing the  $\Delta_{\text{asy-sym}}$  values and potentially allowing for determination of carboxylate coordination.<sup>24,25</sup> Several reports have shown that although there is some value in this method, caution should still be used so as not to reach unfounded conclusions.<sup>25–27</sup> Therefore, the spectra evaluation presented here will be generalized.

The FTIR spectrum of cerium acetate after heating to 230 °C, is shown in Figure 12, along with the difference spectra of

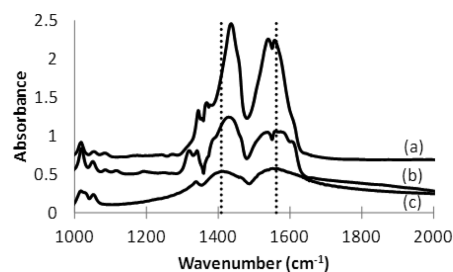


**Figure 12.** FTIR spectra of cerium acetate after (c) heat treatment at 230 °C, (b) ceria difference spectra after exposure to acetic acid at 230 °C, and (a) ceria difference spectra after exposure to acetic acid at 300 °C.

cerium oxide after exposure to small amounts of acetic acid vapor at either 230 or 300 °C. Although only one set of peaks appeared for cerium acetate, it is evident from the figure that the asymmetric peak was split for the ceria compounds. From peak maxima, the  $\Delta_{\text{asy-sym}}$  was found to be equal to  $153 \text{ cm}^{-1}$  for the acetate,  $\Delta_{\text{asy-sym}} = 109/129 \text{ cm}^{-1}$  for the ceria exposed to acetic acid at 230 °C, and  $\Delta_{\text{asy-sym}} = 104/121 \text{ cm}^{-1}$  for the ceria exposed at 300 °C. The acetate value agreed quite well with the previously reported  $\Delta_{\text{asy-sym}}$  of  $150 \text{ cm}^{-1}$  for cerium acetate hydrate, and the  $\Delta_{\text{asy-sym}}$  for ceria exposed to acetic acid at 300 °C was very close to the  $\Delta_{\text{asy-sym}}$  of  $105 \text{ cm}^{-1}$  determined by Hasan et al. after exposure of their ceria catalyst to acetic acid at the same temperature.<sup>11</sup> According to Deacon and Phillips,<sup>21</sup>  $\Delta_{\text{asy-sym}} > 200 \text{ cm}^{-1}$  generally corresponds to unidentate binding,  $\Delta_{\text{asy-sym}} < 150 \text{ cm}^{-1}$  corresponds to bridging or chelating coordination, and  $\Delta_{\text{asy-sym}} < 105 \text{ cm}^{-1}$  is typically more connected to chelation. Although cerium acetate has been reported to have bridging carboxylate bonds, it is unlikely that acetic acid on the surface of ceria could coordinate in a bridging fashion because the bond length between Ce cation pairs is too great.<sup>25,28</sup> Therefore, it is

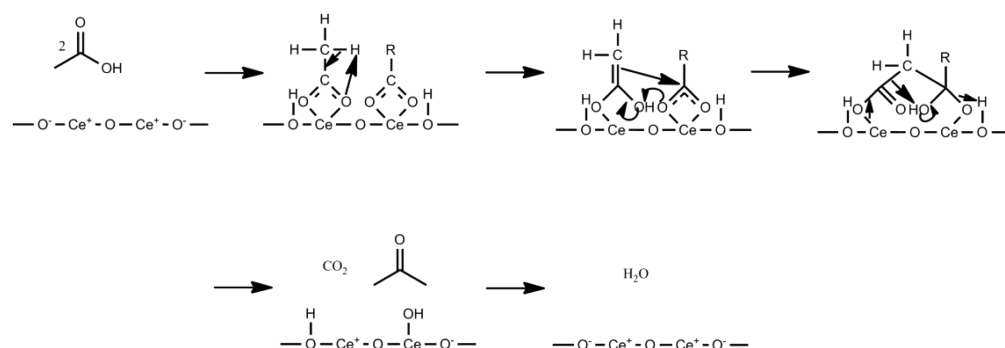


**Figure 13.** Proposed ketonization reaction sequence.

possible that the acid is binding in a chelating fashion on the surface of ceria. Ceria can expose crystallographic facets of {111}, {100}, and {110}, but typically, the {111} surface is prevalent due to its enhanced stability.<sup>29</sup> Because the ideal termination of the {111} surface exposes only cerium with one dangling bond, it seems unlikely that a chelating coordination could occur without surface reconstruction. However, reconstruction of the surface seems quite feasible because Figure 2 shows even bulk crystallite changes can occur given the right conditions.

Carboxylate binding modes may explain some of the phenomena observed with the ceria catalysts that were characterized post reaction. Figure 7 demonstrated that as ceria began to form a bulk carboxylate, the overall macrostructure of the particles was modified toward whisker morphology. The binding of cerium acetate in a bridging arrangement could facilitate this type of elongation, but chelating would not. The different form of metal carboxylate coordination might also help explain the slight differences in Figures 3–5 for cerium acetate and the ceria catalysts used at different temperatures. Ceria used at 230 °C, as would be expected from the XRD results, decomposed in a pattern more closely resembling cerium acetate than did ceria used at 300 °C, since the higher temperature would not allow for bulk acetate formation.

Taken together, the results from the current work suggested a carboxylate mechanism similar to that proposed by Dooley,<sup>17</sup> as shown in Figure 13. This reaction scheme first involves the abstraction of an  $\alpha$ -proton by a carboxyl group bound to a metal. Surface basic sites in a cerium oxyacetate or oxide may also perform this abstraction when available. This difference between the acetate/oxyacetate/oxide system may explain the enhanced stabilities of metal carboxylates observed as shown in Figures 8 and 9. The abstraction step would also be consistent with the reports claiming the necessity of an  $\alpha$ -hydrogen. Branched carboxylates would have greater stability (Figure 11) because the added substituents are electron donors that would lower the acidity. In this mechanism, the reaction would proceed through the formation of a six-membered ring intermediate before the simultaneous formation of CO<sub>2</sub> and acetone, agreeing with Figures 3–5.

Water and carbon dioxide have been commonly cited as inhibitors for the ketonization reaction.<sup>21</sup> This effect would be consistent with the proposed mechanism because water would hydrolyze the carboxylate bonds and carbon dioxide would competitively bind metal sites either in the bulk or on the surface. The proposed mechanism is somewhat similar to that of Pestman et al.<sup>4</sup> in that a proton is initially removed from the

$\alpha$ -carbon on the molecule whose carboxylate group will eventually form carbon dioxide; however, the reaction sequence in Figure 13 would also alleviate concerns that Nagashima et al.<sup>18</sup> expressed about the model by Pestman et al. because the mechanism has the C–C cleavage occurring in the same step as ketone production, thereby prohibiting formation of side product, such as methanol. It is worth noting that the proposed reaction sequence could potentially be generalized to any type of metal oxide ketonization catalyst as well as to being able to occur on the surface or throughout the bulk of the respective material. As such, differences seen between catalysts could be explained through the formation of different types of carboxylate coordination as well as resulting from the electronegativity of the respective metal, creating discrepancies as to the ease in which the C–C bond is broken. The strength of the M–O bonds in the metal oxide is also important in the proposed mechanism. Strong M–O bonds would make formation of the needed metal carboxylate groups difficult, whereas weak M–O bonds would result in the formation of thermally stable metal carboxylates.

### 3. CONCLUSIONS

Characterization techniques such as XPS, SEM, FTIR, and XRD of fresh and spent ceria catalysts were found to be necessary to explain some of the phenomena, such as cerium reduction and morphology changes, seen in this work as well as in previous reports on the ketonization reaction. Degradation of the ceria crystal structure was found to be dependent on the temperature regime used for the ketonization reaction. Therefore, the long postulated belief that ketonization with ceria occurs through multiple catalytic routes, based upon observance of a bulk carboxylate phase, does not need to be invoked. A mechanism involving the coupling of two carboxylate species, either on the surface or throughout the bulk, would explain the results observed in the current work as well as experimental results given in previous work by other groups. The postulate that pyrolytic decomposition of carboxylates is the primary mechanism for ketonization provides a direction for developing improved catalytic materials. Although the postulated ketonization reaction sequence can be extended to explain results for a range of metal oxides, further investigations into ketonization catalysts are needed, particularly with respect to more complex systems, such as supported metal oxides or mixed metal oxides.

## ■ ASSOCIATED CONTENT

### ■ Supporting Information

Figures S1–S3 showing the XRD, XPS, and SEM image of the fresh ceria. In situ XRD of ceria exposed to acetic acid vapors at 300 °C in Figure S4. Figures S5 and S6 showing SEM image and XPS of ceria after exposure to pivalic acid. This material is available free of charge via the Internet at <http://pubs.acs.org>.

## ■ AUTHOR INFORMATION

### Corresponding Author

\*E-mail: [bshanks@iastate.edu](mailto:bshanks@iastate.edu).

### Notes

The authors declare no competing financial interest.

## ■ ACKNOWLEDGMENTS

This work was funded by the National Science Foundation through PIRE (OISE 0730227) and ERC (EEC-0813570) grants. Jim Anderegg (Ames Laboratory) was very kind in helping with the XPS results. Dan Weis, an ISU undergraduate, also helped perform some of the experiments.

## ■ REFERENCES

- (1) Bridgwater, A. V. *Biomass Bioenergy* **2012**, *38*, 68–94.
- (2) Czernik, S.; Bridgwater, A. V. *Energy Fuels* **2004**, *18*, 590–598.
- (3) Kunkes, E. L.; Simonetti, D. A.; West, R. M.; Serrano-Ruiz, J. C.; Gartner, C. A.; Dumesic, J. A. *Science* **2008**, *322*, 417–421.
- (4) Pestman, R.; Koster, R. M.; van Duijne, A.; Pieterse, J. A. Z.; Ponec, V. J. *Catal.* **1997**, *168*, 265–272.
- (5) Rajadurai, S. *Catal. Rev.: Sci. Eng.* **1994**, *36*, 385–403.
- (6) Yakerson, V. I.; Fedorovskaya, E. A.; Klyachko-Gurvich, A. L.; Rubinshtein, A. M. *Kinet. Katal.* **1961**, *2*, 907–915.
- (7) Mekhemer, G. A. H.; Halawy, S. A.; Mohamed, M. A.; Zaki, M. I. *J. Catal.* **2005**, *230*, 109–122.
- (8) Lide, D. R. *CRC Handbook of Chemistry and Physics*; CRC Press LLC: Boca Raton, 2003–2004.
- (9) Gliniski, M.; Kijenski, J.; Jakubowski, A. *Appl. Catal., A* **1995**, *128*, 209–217.
- (10) Gaertner, C. A.; Serrano-Ruiz, J. C.; Braden, D. J.; Dumesic, J. A. *J. Catal.* **2009**, *266*, 71–78.
- (11) Deng, L.; Fu, Y.; Guo, Q.-X. *Energy Fuels* **2009**, *23*, 564–568.
- (12) Kobune, M.; Sato, S.; Takahashi, R. *J. Mol. Catal. A: Chem.* **2008**, *279*, 10–19.
- (13) Yamada, Y.; Segawa, M.; Sato, F.; Kojima, T.; Sato, S. *J. Mol. Catal. A: Chem.* **2011**, *346*, 79–86.
- (14) Snell, R. W.; Shanks, B. H. *Appl. Catal., A* **2013**, *451*, 86–93.
- (15) Hasan, M. A.; Zaki, M. I.; Pasupulety, L. *Appl. Catal., A* **2003**, *243*, 81–92.
- (16) Dooley, K. M. Catalysis of Acid/Aldehyde/Alcohol Condensations to Ketones. In *Catalysis*; Spivey, J. J., Roberts, G. W., Eds.; The Royal Society of Chemistry, Cambridge, 2004, pp 293–319.
- (17) Friedel, C. *Justus Liebigs Ann. Chem.* **1858**, *108*, 122–125.
- (18) Nagashima, O.; Sato, S.; Takahashi, R.; Sodesawa, T. *J. Mol. Catal. A: Chem.* **2005**, *227*, 231–239.
- (19) Rubinshtein, A. M.; Slinkin, A. A.; Yakerson, V. I.; Fedorovskaya, E. A. *Russ. Chem. Bull.* **1961**, *10*, 2090–2092.
- (20) Gangadharan, A.; Shen, M.; Sooknoi, T.; Resasco, D. E.; Mallinson, R. G. *Appl. Catal., A* **2010**, *385*, 80–91.
- (21) Gaertner, C. A.; Serrano-Ruiz, J. C.; Braden, D. J.; Dumesic, J. A. *J. Catal.* **2009**, *266*, 71–78.
- (22) Rajadurai, S.; Kuriacose, J. C. *Mater. Chem. Phys.* **1987**, *16*, 17–29.
- (23) Mehrotra, R. C.; Bohra, R. *Metal Carboxylates*; Academic Press: London, 1983.
- (24) Nakamoto, K.; Fujita, J.; Tanaka, S.; Kobayashi, M. *J. Am. Chem. Soc.* **1957**, *79*, 4904–4908.
- (25) Deacon, G. B.; Phillips, R. J. *Coord. Chem. Rev.* **1980**, *33*, 227–250.
- (26) Edwards, D. A.; Hayward, R. N. *Can. J. Chem.* **1968**, *46*, 3443.
- (27) Deacon, G. B.; Huber, F.; Phillips, R. J. *Inorg. Chim. Acta* **1985**, *104*, 41–45.
- (28) Stubenrauch, J.; Brosha, E.; Vohs, J. M. *Catal. Today* **1996**, *28*, 431–441.
- (29) Baudin, M.; Wójcik, M.; Hermansson, K. *Surf. Sci.* **2000**, *468*, 51–61.